WARSAW UNIVERSITY OF TECHNOLOGY Index 351733
FACULTY OF CIVIL ENGINEERING
COMMITTEE FOR CIVIL AND WATER ENGINEERING
POLISH ACADEMY OF SCIENCES ISSN 1230-2945

DOI: 10.24425/ace.2026.1408

ARCHIVES OF CIVIL ENGINEERING

Vol. LXXII ISSUE 3 2026

 pp. 493 – 508

Research paper

A flat type anchorage system for short tendons with low prestress wedge draw-in loss

Ruizhu Tian[1], Li Zhu[2], Yonghu Yao[3], Yanwu Zhi[4], Wei Liu[5], Hongsheng Huang[6]

Abstract: Currently, there are drawbacks to the prestressing anchorage products used in prestressed concrete bridges, including significant anchorage draw-in during tensioning, inconveniences during construction, anchorage failure during usage, and operation subject to human interference. In order to overcome these unfavorable factors, a flat low draw-in anchorage system was developed through scheme design, selection, finite element analysis and trial production test. By adjusting the jacking force, this method uses a wedge-shaped structure in the shape of a jacking pad to guarantee that the draw-in value is within 1 mm. Slow bevelled contact, which has high self-locking properties and improves the contact surface while lowering compressive stress, is used between the pad plate and the flat low draw-in anchorage plate at a small angle of rise. Through the structural form of jacking the mat plate, jacking it into place at one time, and quantitatively controlling the value of jacking force, the system achieves standardized construction and reduces errors in human operation. The wedge anchorage system performs exceptionally well in terms of safety under simulated operating conditions, according to finite element analysis. After the fatigue test verification study, there was no fatigue damage to the anchorage parts, and the prestressed tendons were not broken. In the meantime, the sealing test revealed that there was no breakage of the anchorage's components, and that there were no leaks or water stains inside the tendons or the anchoring itself. This system offers a solid assurance against girder deflection, web cracking in pre-stressed concrete bridges, and other ailments.

Keywords: bridge engineering, prestressed anchorage, flat tendon, anchoring system, prestress loss

[1]MSc., Eng. Cand., School of Civil Engineering, Beijing Jiaotong University, Beijing 100044, China, e-mail: 24120990@bjtu.edu.cn, ORCID: 0009-0004-0347-2924
[2]Prof., PhD., Eng., School of Civil Engineering, Beijing Jiaotong University, Beijing 100044, China, e-mail: zhuli@bjtu.edu.cn, ORCID: 0000-0001-9736-6137
[3]B.Eng., LiuZhou Qiaosha Technology Development Co., Ltd, Liuzhou Guangxi 545007, China, e-mail: 1119693112@qq.com, ORCID: 0009-0005-2030-089X
[4]MSc., Eng., China Railway Design Corporation, Tianjin 300142, China, e-mail: zhiyanwu@crdc.com, ORCID: 0009-0005-8501-6961
[5]PhD. Cand., School of Civil Engineering, Beijing Jiaotong University, Beijing 100044, China, e-mail: 23111340@bjtu.edu.cn, ORCID: 0000-0003-0214-5206
[6]B.Eng., LiuZhou Qiaosha Technology Development Co.,Ltd, Liuzhou, Guangxi 545007, China, e-mail: 2373163668@qq.com, ORCID: 0009-0001-7514-7328

1. Introduction

One of the main elements influencing the longevity and performance of prestressed structures is prestress loss [1, 2]. The long-term safety and stability of the structure will be greatly impacted by prestress losses in bridge engineering, particularly in the design and implementation of highway and railroad bridges [3]. Prestress loss is often separated into two categories: immediate loss and long-term loss [4]. The friction force, slip effect, and anchorage draw-in during the tensioning process are the primary causes of the immediate loss [5]. Concrete shrinkage, creep, temperature changes, and steel bar relaxation are all intimately linked to long-term losses [6–9].

Commonly used anchorages in traditional prestressed systems, like circular anchorages, flat anchorages, and finished rolled rebar anchorages [10], are highly utilized in engineering. However, their high draw-in (typically 3–5 mm) will result in a significant loss of applied prestress, particularly in short-beam prestressed systems. An efficient solution to this issue is the introduction of low draw-in anchoring. Through design optimization, the anchoring enhances operability and safety during construction while also reducing draw-in.The following issues still plague commonly used prestressed short beams in the actual construction process: nut-type circular low draw-in anchorage and prestressing tendon anchorage: because the nut is in the center of the anchorage, the space in the tension slot is very inconvenient, and workers find it difficult to tighten the nut, which makes it difficult to meet the design requirements of low draw-in. This is because the manual operation error is large and the vertical prestress efficiency is challenging to ensure due to the difficulty of tightening the nut during the prestressed tension of the rebar. Reducing the prestress loss of short beams and maintaining technical quality are critical.

Hou et al. [11] proposed a novel CFRP steel strand bundle anchoring system, demonstrated its mechanical characteristics, and confirmed its anchoring effectiveness through experimental research and mechanical analysis. This gave theoretical backing and an empirical foundation for resolving the issue of stress concentration at the conventional anchoring interface. According to research by Shao et al. [12–15], low draw-in anchorage can effectively compensate for draw-in loss for shorter prestressing strands; the impact of low draw-in prestressing anchorage on concrete is the same as that of ordinary anchorage; and the reliability of the vertical prestressing system of low draw-in strand is significantly higher than that of fine-rolled rebar. The performance of RC slabs reinforced with prestressed CFRP strips was experimentally examined by Correia et al. [16] utilizing a variety of anchoring system backgrounds. Using high-performance fiber- reinforced self-compacting concrete (HPFRC) in the anchorage range saves material and lowers the density of reinforcement in the vicinity of the local anchorage zones, according to Marchão et al. [17] investigation of the prestress transfer pattern in the top and web plates of box girders.

The selection and manufacturing precision of anchorage are the most crucial factors in prestressing loss, according to research and practice. Controlling prestressing construction methods comes in second. This paper proposes a flat low draw-in anchorage system that can be adjusted by the supporting automatic tooling. The anchorage system is proven to be effective in guaranteeing the low draw-in of prestressing force in short beams after the actual test. This is done by combining the design of flat tendons with the advanced flat anchorage technology to reduce the loss of prestressing force in short beams.

2. Program design and selection

The structural type of the flat low draw-in anchorage system is determined to be tension end-prestressing tendon-fixed end based on the product's performance, safety, operability, and other requirements; main objects of the study are the anchorage at the tension end, prestressing tendon structure, the anticorrosion system structure, and the special construction tooling. The schematic diagram in Fig. 1 illustrates this structure. The prestressing tendon may be an unbonded strand, bonded strand (grouting is necessary), or another structure. The fixed end of the pre-stressing tendons can take on various structural forms based on the actual demand. These include the standard wedge-type anchorage, grip-wrapped anchorage (as shown in Fig. 2), embossed anchorage, and the flat low draw-in anchorage that is the subject of this system. The pre-stressing tendons can be bonded strands (which require grouting), unbonded strands, or other structural forms of tendons.

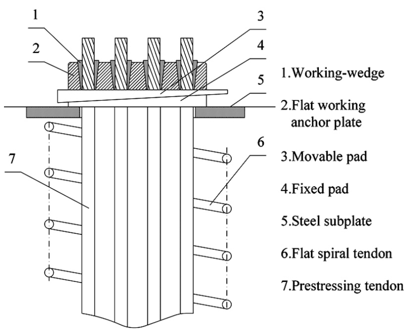

Fig. 1. Schematic diagram of the tension end structure of the flat low draw-in anchorage system

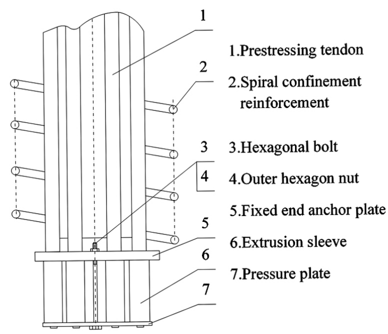

Fig. 2. Schematic diagram of the grip-wrapped fixed end structure

In order to achieve low draw-in, the concrete member must first be subjected to tensile stress through the prestressing component, which will put it in a state of pre-added stress. In the second tensioning, the clamping piece, the working anchorage plate, and the prestressing tendon are lifted together, creating a gap between the working anchorage plate and the anchorage pad. To fill this gap and achieve the low draw-in adjustment of the anchorage, the movable pad is pushed forward.

2.1. Principle of operation of low draw-in compensation

Draw-in compensation can be achieved by using a threaded vice, according to the previously indicated research status of low draw-in anchorage. Based on the original anchorage components, the anchorage plan uses additional structural measures to achieve the basic idea of compensating draw-in. By increasing compensation measures, it is possible to not only utilize the original, dependable, and mature anchorage fixture technology, but also to lessen the difficulty of the study by requiring only a local study to accomplish the goal and to ensure a better technical economy.

The use of oblique flat pads in the form of a structure results in two flat pads with the same inclination angle and a slope of the relative assembly. The height of the pad combination increases as the flat pads move in the direction of one another, and decreases as they move away from one another.

The tensioning end anchorage is formed by the strand connecting the anchoring and the bevelled flat combination in series. Set in the lower portion of the flat mat for the fixed flat mat, which has a through-hole with prestressing tendons through it; placed in the upper portion of the flat mat for the activity of the flat mat, which has a long groove with prestressing tendons through it; the activity can take place either before or after the activity. In Fig. 3, the flat construction is displayed.

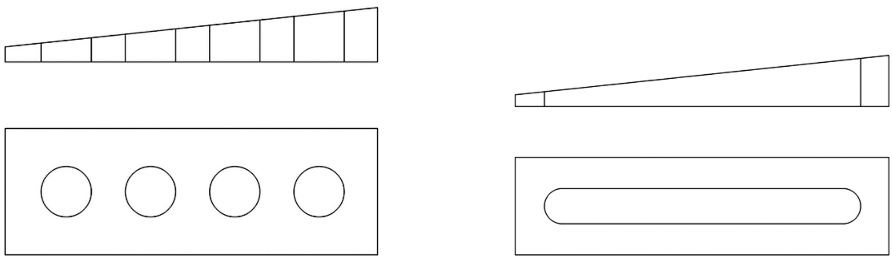

(a) (b)

Fig. 3. Schematic diagram of the wedge structure; (a) Fixed pad, (b) Movable pad

As seen in Fig. 4 below, the particular execution of the pre-established scheme can be separated into two distinct structural schemes: scheme a, which combines a flat block and a beveled angle on the working anchorage plate, and scheme b, which combines two flat blocks.

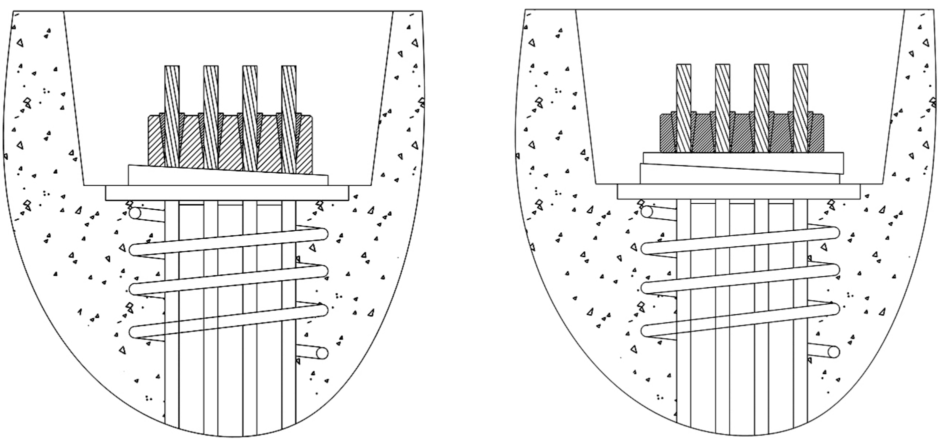

(a) (b)

Fig. 4. Wedge combination scheme; (a) Scheme a, (b) Scheme b

Table 1 displays a comparison of the two structural systems' benefits and drawbacks.

Table 1. A comparison of the two structural schemes

Serial number	Capability item	Flat combination scheme a	Flat combination scheme b
1	Structural complexity	Superior	Mid
2	Installation operation convenience	Superior	Mid
3	Adjustability	Non-control	Adjustable
4	Change the original anchorage fixture	Need to change	No change

Following comparison, scheme b is suggested for this anchorage's implementation. The flat mat at the top is movable, with long grooves set on it that allow the prestressing tendons to pass through and be moved; the flat mat at the bottom is fixed, with through holes laid according to the number of prestressing tendons, and the tendons pass through the through holes. The adjustment device is susceptible to the vertical pressure from the working anchorage plate and the anchorage pad reaction force of the joint action. It is composed of both fixed and movable pads, with the fixed and movable pads having an angle of β. Fig. 5 below illustrates the structure of a regulating device made up of both fixed and moveable flat pads.

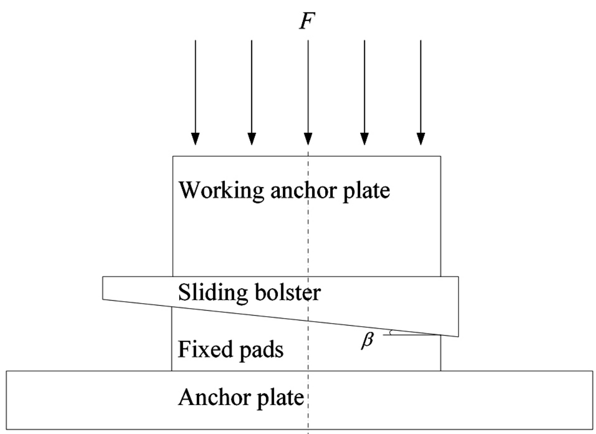

Fig. 5. Schematic diagram of the regulating device structure

2.2. Self-locking analysis

The slope block force is depicted in Fig. 6 below. When $f = F_2$, the item may remain static because the static friction force is equal to the thrust of the object.

F gravity, F' normal response force, F_1 positive pressure, F_2 thrust, and f friction are a few of them.

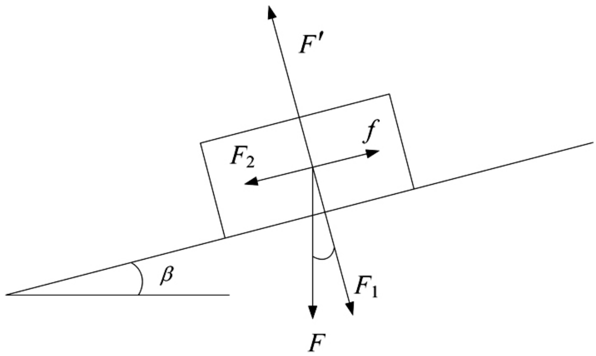

Fig. 6. Schematic diagram of the inclined block

The static friction coefficient between steel parts and steel parts is $\mu = 0.15$; the maximum static friction force is μF_1, and the maximum inclination angle β is 8.5°, which is 1.2 times the safety factor. At this time, $\beta \le 7°$. When the angle of the adjusting device is less than or equal to 7°, complete self-locking can be achieved. In order to further ensure the anchorage performance of the device, the angle of the device is adjusted to 6°. The adjustment device and the anchorage are installed in series by prestressed tendons, as shown in Fig. 1.

2.3. The installation relationship between the adjusting device, the anchorage fixture and the prestressed tendon

By manually rotating the nut, the current threaded vice draw-in compensation measures are in the second tension to attain the desired value. As seen in Figs. 7 and 8, this system draw-in is accomplished for the hydraulic jacking workpiece by utilizing a specialized hydraulic jack to finish the jacking pad's activity. After releasing the tension, the low draw-in compensation operation is finished.

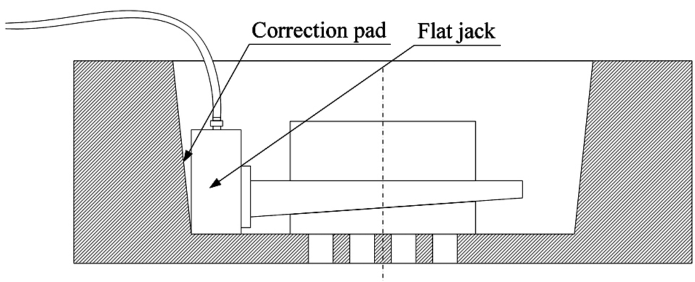

Fig. 7. Schematic diagram of the special jack push Fig. 8. Special oil pressure jack jacking device

Fig. 8. Special oil pressure jack jacking device

3. Stress analysis of regulating device

3.1. Material selection and mechanical property determination of the regulating device

The movable pad and the fixed pad adopt 40Cr in GB/T 3077-2015 "Alloy structure steels" [17], and its yield strength is 785 MPa. That is, $[\sigma]_{40\mathrm{Cr}} = 785$ MPa. The anchor plate material is Q235 in GB/T 700-2006 "Carbon structural steels" [18], and its yield strength is 235 MPa; that is, $[\sigma]_{\mathrm{Q235}} = 235$ MPa. The material of working anchor plate is 40Cr. The safety factor of mechanical properties of materials is 1.2, so the allowable compressive stress of 40Cr and Q235 materials in this scheme is: $785/1.2 = 654$ MPa; that is, $[\sigma]_{\mathrm{j40Cr}} = 654$ MPa. The allowable compressive stress of Q235 is $235/1.2 = 195.8$ MPa; that is, $[\sigma]_{\mathrm{jQ235}} = 195.8$ MPa. The nominal breaking force of ϕ15.24–1860 steel strand is 260 kN, and the actual tensile force is 0.75 times that of $0.75 \times 260 = 195.3$ kN.

3.2. Finite element modeling and analysis results

Numerical simulation is done with UG NX8.5 software. Fig. 9 displays the finite element analysis of the fixed plate, anchorage plate, and moving plate with various holes. The ideal steel elastic-plastic model is depicted in Fig. 10, where the elastic modulus (E_S) is 2.05×10^5 MPa, the yield strength σ_{S} is the yield strength, and the precise value of each material's yield strength is explained in 2.1.The anchorage plate's bottom serves as the boundary condition; there is a contact relationship between the anchorage plate and the movable plate as well as between the moveable plate and the fixed plate. The end face of the fixed plate receives a consistent load, the adjustment device's angle is set at 6 degrees, and the friction coefficient is set at the standard value of 0.15.

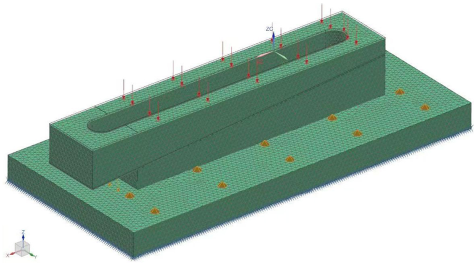

Fig. 9. Finite element model diagram

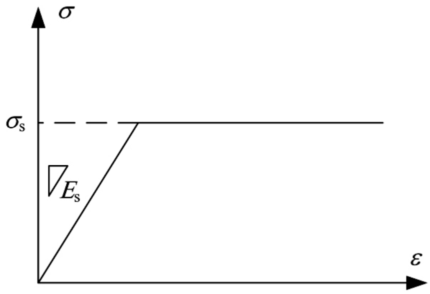

Fig. 10. The ideal elastoplastic model

Figs. 11–13 display the stress cloud diagram of finite element analysis, while Tables 2–4 display the findings. When the maximum stress value is determined by the peak stress σ_{Max} – software, where the total load F is the total load applied by the anchorage. The stress value is very high since each local structure in the theoretical model will produce stress concentration throughout the computation. The larger stress mean σ item is used as the criterion to judge whether the stress meets the standard; for instance, a large concentrated stress will be generated at the contact ring position between the anchorage plate and the anchorage plate, so the "peak stress" is not used as an item to determine whether the stress meets the requirements; the bigger stress uniformity value is the estimated value of the larger portion of the stress in the major stress component's stress distribution map, based on the computation results.

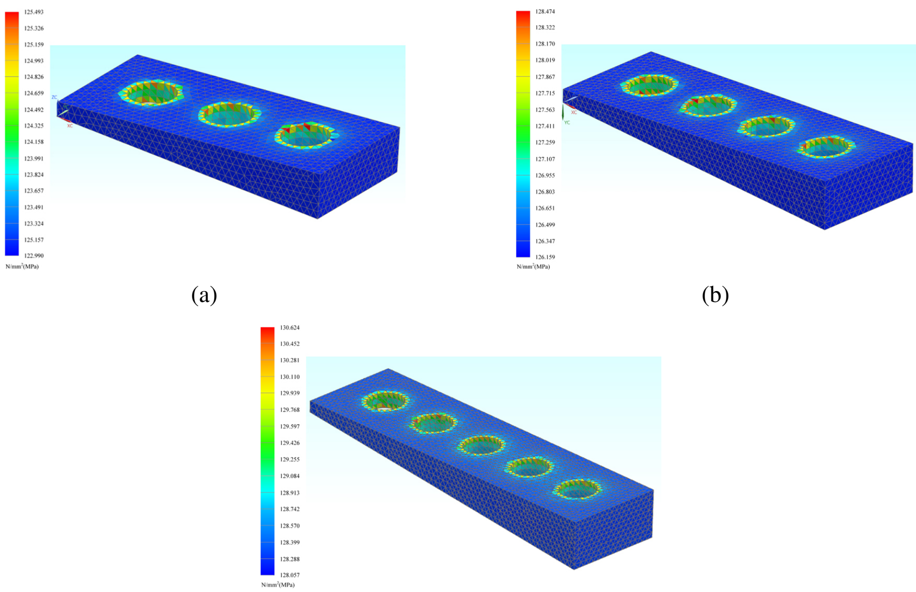

(a) (b) (c)

Fig. 11. Fress stress analysis of fixed pad; (a) Model with 3 holes, (b) Model with 4 holes, (c) Model with 5 holes

Table 2. Finite element analysis results of fixed pads

Specification	Total load F (kN)	Peak stress σ_{Max} (MPa)	Larger mean stress σ (MPa)	Criterion for judgement $[\sigma]_{\text{j40Cr}} = 654$ MPa	Security judgement
Model with 3 holes	585.9	125.493	123.0	$\sigma \leq [\sigma]_{\text{j40Cr}}$	Qualification
Model with 4 holes	781.2	128.474	126.3	$\sigma \leq [\sigma]_{\text{j40Cr}}$	Qualification
Model with 5 holes	976.5	130.624	128.3	$\sigma \leq [\sigma]_{\text{j40Cr}}$	Qualification

Table 3. FEM analysis results of movable pads

Specification	Total load F (kN)	Peak stress σ_{Max} (MPa)	Larger mean stress σ (MPa)	Criterion for judgement $[\sigma]_{\text{j40Cr}} = 654$ MPa	Security judgement
Model with 3 holes	585.9	162.16	152.9	$\sigma \leq [\sigma_1]$	Qualification
Model with 4 holes	781.2	167.60	160.1	$\sigma \leq [\sigma_1]$	Qualification
Model with 5 holes	976.5	171.38	162.7	$\sigma \leq [\sigma_1]$	Qualification

Notes: The area under stress is along the thin edge.

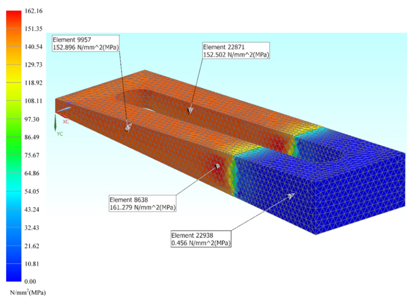

(a)

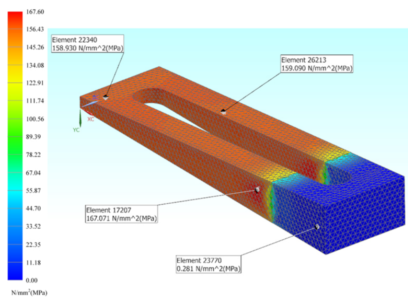

(b)

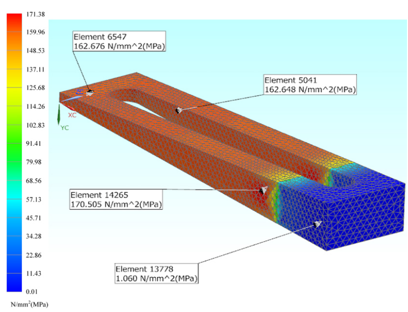

(c)

Fig. 12. Fad stress cloud map of the movable pad; (a) Model with 3 holes, (b) Model with 4 holes, (c) Model with 5 holes

Table 4. Finite element analysis results of anchorage plates

Specification	Total load F (kN)	Peak stress σ_{Max} (MPa)	Larger mean stress σ (MPa)	Criterion for judgement $[\sigma]_{\text{jQ235}} = 195.8$ MPa	Security judgement
Model with 3 holes	585.9	122.72	90.8	$\sigma \leq [\sigma]_{\text{jQ235}}$	Qualification
Model with 4 holes	781.2	126.55	97.5	$\sigma \leq [\sigma]_{\text{jQ235}}$	Qualification
Model with 5 holes	976.5	128.51	114.3	$\sigma \leq [\sigma]_{\text{jQ235}}$	Qualification

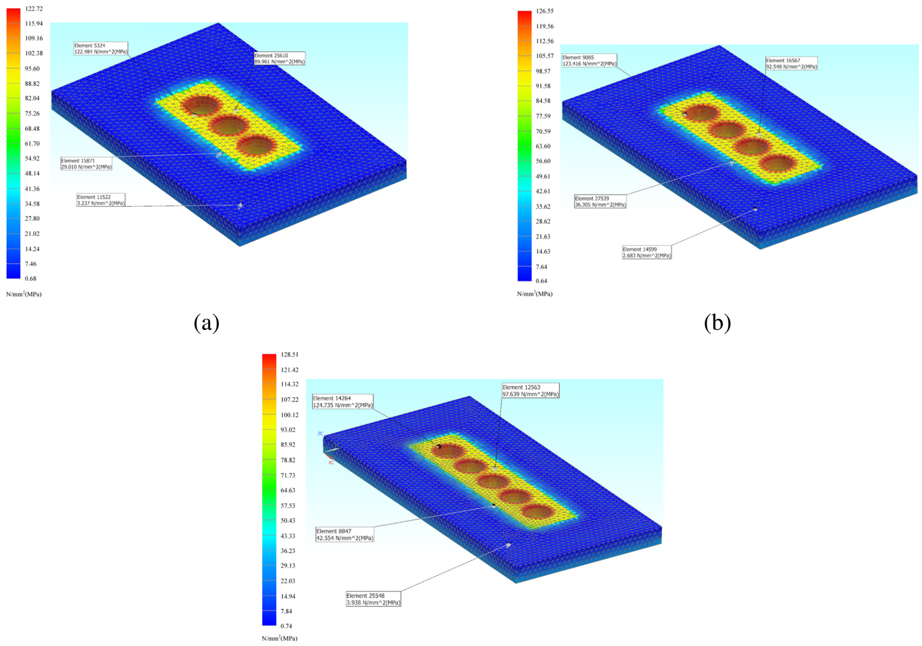

(a) (b) (c)

Fig. 13. The cloud diagram of finite element analysis of anchorage plate; (a) Model with 3 holes, (b) Model with 4 holes, (c) Model with 5 holes

4. Testing for performance of low draw-in anchorage system

4.1. Fatigue test

The fatigue test (Fig. 14) is carried out on the fatigue testing machine. When the load capacity of the testing machine is limited, the number of actual anchorage prestressed tendons can be reduced according to the representative principle of the test results or the test assembly can be constructed by using the same series of small-sized anchorages, but the effective anchorage unit should not be less than 1/2 of the standard configuration. The test loading program requires loading to the upper limit of stress at a rate of about 100 MPa/min. After the stress amplitude is stable, the cycle counting is started, and the dynamic loading frequency must be controlled within 500 times min. The system needs to be verified by 2×10^6 cyclic loads. The upper limit of the test stress is 65% of the tension control stress of the prestressed tendon, and the stress amplitude should not be less than 100 MPa. The acceptance standard stipulates that after 2×10^6 cyclic loads, the anchor assembly shall not have fatigue damage, and the cumulative cross-sectional area of fatigue fracture caused by the anchorage clamping effect of the prestressed tendon shall not exceed 5% of the total cross-sectional area of the specimen. In this scheme, a test model was constructed for four-hole anchors, and the dynamic fatigue load parameters were set as upper limit 677.04 kN (corresponding to 65% tension control stress) and lower limit 621.04 kN, forming a cyclic loading system with an amplitude of 56 kN, until 2×10^6 cycles or specimen failure termination tests were completed. The test items of this sample meet the requirements of the standard of TB/T 3193-2016 "Anchorage, grip and coupler for prestressing tendons in railway construction" [20].

Fig. 14. Fatigue test

4.2. Leak test

The primary goal of the sealing test (Fig. 15) is to evaluate the unique technical performance of prestressed tendons without grouting, such as flat tendon bodies, slowly condensed steel strands, or unbonded steel strands, under exceptional corrosion resistance conditions. The anchorage assembly remained intact after 10 axial dynamic load cycles, an 8×24-hour temperature cycle, and 4×250 transverse dynamic load cycles. Additionally, neither the tendon body nor the inside of the anchorage were stained with colored water, nor were there any leaks or water stains. The sample's sealing ability satisfies the standards set out in the JT/T 771-2009 "Technical conditions for unbonded steel strand stay cable" standard [21].

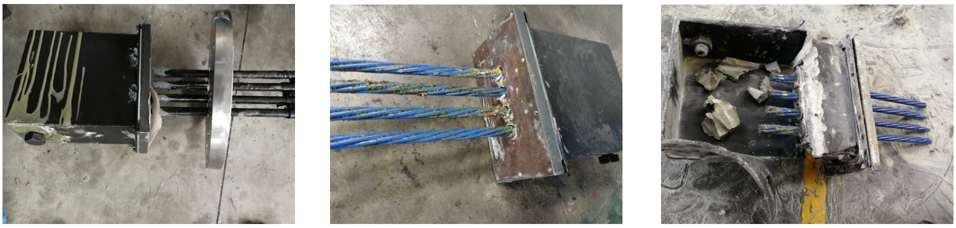

(a) (b) (c)

Fig. 15. Observation images during the test; (a) Removed anchorage and tendon body after dynamic load test, (b) Peel off the tendon body PE layer, (c) Open the protective cover

5. Flat tendon low draw-in anchorage system

5.1. Advantages of flat tendon body

When the 2-5 porous prestressed tendons are fixed, it is necessary to strictly conform to the design position and maintain the relative position, spacing and spatial angle, so as to avoid adverse deformation such as torsion and folding angle, as shown in Fig. 16(a). However, in practical engineering, the complex steel mesh and pouring mold often make the reinforcement requirements difficult to meet. Therefore, it is necessary to optimize the prestressed reinforcement structure to simplify the reinforcement fixing process. Reducing the angle of the reinforcement and reducing the bonding effect of the concrete can effectively reduce the prestress loss, as shown in Fig. 16(b).

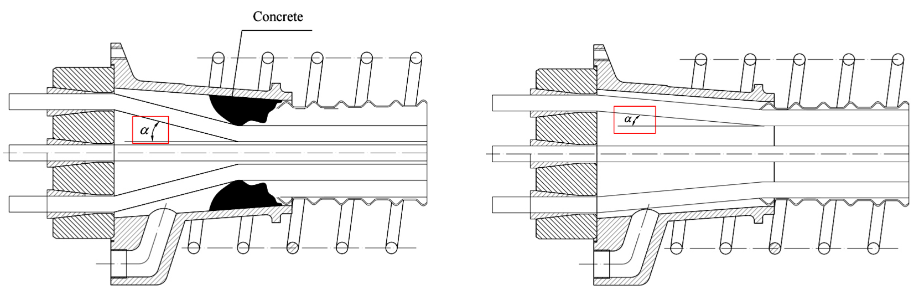

(a) (b)

Fig. 16. Effect position of prestressed tendons; (a) Schematic diagram of local concrete influence, (b) Schematic diagram of the prestressed reinforcement folding angle

The unbonded prestressed tendon used in this scheme is formed by hot extrusion PE after the surface of the steel strand is coated with oil. The flat tendon body is optimized on this basis, and a connecting fixed structure is set between two or more strands (as shown in Fig. 17). During the construction of the flat anchorage system, the prestressing tendons should be fixed in the design position in advance to ensure that there is no displacement during the concrete pouring and vibrating process, so as to avoid affecting the prestressing effect or retaining the hidden danger of quality.

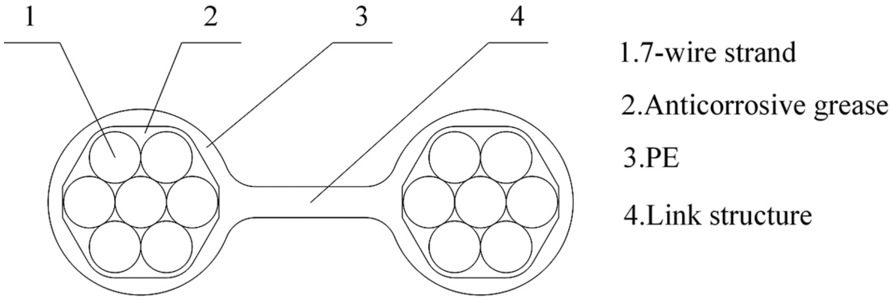

Fig. 17. Flat tendon body structure

Compared with the multi-strand single tendon body, the flat tendon body has fewer fixed points, which significantly reduces the time and complexity of the fixed operation. The single tendon body needs to be fixed one by one at many places, which is easy to cause the deviation of the position and spacing of the reinforcement, especially the angle at the entrance of the anchor plate is difficult to control and the force is uneven. The flat tendon body keeps the fixed interval consistent through the integrated design to ensure the accurate entrance angle and uniform force, and the tendon is convenient to wear and avoid winding, which ensures the mechanical performance of the tendon body. In addition, attention should be paid to the anti-corrosion of flat tendon bodies, and effective protective measures should be taken to ensure long-term stability and durability.

5.2. Protection measures against corrosion

5.2.1. Anticorrosion selection

The anchorage components include embedded parts and tensioning assemblies. For embedded parts, temporary anti-corrosion measures are adopted, as they only need to remain rust-free during storage and transportation to meet usage requirements. The tensioning assemblies is composed of anchor plate, adjusting device and working wedge. Anchor plates and wedges are very mature prestressed products, and anti-corrosion measures are also mature. Among them, the anchor plate has two ways of bluing treatment and zinc plating. The anti-corrosion technology is mainly bluing, and the anti-corrosion of the wedge is still based on the application of anti-corrosion grease as the mainstream anti-corrosion measure.

5.2.2. Anticorrosion of the system during construction

a. Anti-corrosion of prestressing tendons after pre-embedding and before the first tensioning

The prestressed tendon used in the flat low retraction anchorage system is unbonded prestressed tendon or flat tendon body. The protective measures are as follows: (1) Before tension, the outer anticorrosive material of the exposed unbonded tendon or flat tendon body is not peeled off temporarily, and then peeled off when tension; (2) The plastic protective cap is installed at the end of the prestressed tendon (as shown in Fig. 18) to prevent water vapor from invading from the end and corroding the prestressed tendon.

Fig. 18. Protective cap (left), unbonded prestressed tendon (middle), and unbonded tendons of the protective cap (right)

b. Preventing corrosion prior to tensioning and sealing the anchorage

Due to the necessity of performing multiple tensioning and cleaning procedures to remove excess prestressing tendons and other operations, as well as the effects of the construction site environment, the entire anchorage surface can be covered with plastic film prior to the initial tensioning and anchorage sealing. This will prevent rainwater from soaking the anchorage and causing corrosion.

5.2.3. Anchorage sealing anti-corrosion

Before sealing the anchor, 2-3 mm special anticorrosive grease is applied to the surface of the wedge and the exposed prestressed tendon, and then the protective cap is set up. The length of the protective cap needs to completely cover the exposed part of the prestressed tendon and the wedge to prevent the overflow of grease and isolate the epoxy mortar and grease. Because the water and air erosion resistance of epoxy mortar is better than that of concrete, epoxy mortar is selected as the sealing material of the anchor. The third-party water tightness test (as shown in Figure 19) showed that after 192 hours of sealing test, there was no water trace erosion in the sealing area.

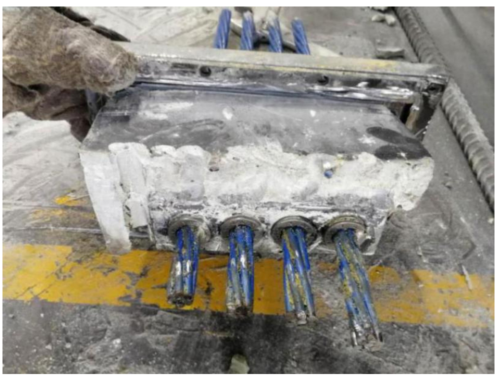

Fig. 19. Seal performance test of epoxy mortar sealing anchorage

6. Conclusions

In view of the increasing demand for anchorage in the construction of highways, railways and municipal bridges in China, a flat anchorage system that can realize low retraction of prestressed steel strands is developed. The system has been successfully applied to a cable-stayed bridge in Jiangxi Province, which effectively solves the diseases such as web cracking and beam deflection of prestressed concrete bridges, and shows broad market application potential. The details are as follows:

1. Through creative design, the first flat anchorage system that achieved minimal draw-in of prestressing strands (draw-in of 0.5-0.7 mm) was created. This system uses cutting-edge flat anchoring technology, which enhances anchorage stability and overall structural dependability while drastically reducing strand draw-in during tensioning.
2. The finite element analysis results show that the flat anchorage system exhibits excellent safety performance under simulated working conditions, and can effectively withstand the design load during the anchorage process of prestressed steel strands without accidental deformation or failure.
3. The invented low retraction anchorage system of flat tendon body adopts unbonded prestressed steel strand or flat tendon body to optimize the tendon-piercing process. The flat tendon structure avoids winding during tendon installation, reduces installation difficulty and improves construction efficiency.

Acknowledgements

The research was financially supported by the Eighth National "Ten Thousand Talents Plan for Top Young Talents" of China and the National Natural Science Foundation of China (No. 52478117, No. 52378120), for which the authors are gratefully acknowledged.

References

[1] T. Guo, Z. Chen, S. Lu, and R. Yao, "Monitoring and analysis of long-term prestress losses in post-tensioned concrete beams", *Measurement*, vol. 122, pp. 573–581, 2018, doi: 10.1016/j.measurement.2017.07.057.

[2] G.R. Lu, Q.B. Wang, X.J. Li, and L.G. Wang, "Study and Practice of Controlling Anchorage Force Loss of Prestressed Anchor Rope", *Applied Mechanics and Materials*, vol. 166-169, pp. 1663–1668, 2012, doi: 10.4028/www.scientific.net/AMM.166-169.1663.

[3] P.M. Páez and B. Sensale, "Improved prediction of long-term prestress loss in unbonded prestressed concrete members", *Engineering Structures*, vol. 174, pp. 111–125, 2018, doi: 10.1016/j.engstruct.2018.07.038.

[4] T. Lou, S.M.R. Lopes, and A.V. Lopes, "A finite element model to simulate long-term behavior of prestressed concrete girders", *Finite Elements in Analysis & Design*, vol. 81, pp. 48–56, 2014, doi: 10.1016/j.finel.2013.11.007.

[5] G.H. Cao, C. Han, Y. Dai, and W. Zhang, "Long-Term Experimental Study on Prestressed Steel-Concrete Composite Continuous Box Beams", *Journal of Bridge Engineering*, vol. 23, no. 9, art. no. 04018067, 2018, doi: 10.1061/(ASCE)BE.1943-5592.0001269.

[6] Z. Huang et al., "Long-term deformation and prestress loss of PRC beam under vari-humidity environment: Preliminary experiments and multi- scale simulations", *Engineering Structures*, vol. 322, Part A, art. no. 119122, 2025, doi: 10.1016/j.engstruct.2024.119122.

[7] Z.P. Bažant and Q. Yu, "Relaxation of Prestressing Steel at Varying Strain and Temperature: Viscoplastic Constitutive Relation", *Journal of Engineering Mechanics*, vol. 139, no. 7, pp. 814–823, 2013, doi: 10.1061/(ASCE)EM.1943-7889.0000533.

[8] F. Xie, T. Chang, C. Zhang, F. Zhang, G. Kuang, and Y. Zhang, "Medium and short-term effective prestress losses considering multiple factors: Laboratory and on-site beam experiments", *Structures*, vol. 68, art. no. 107166, 2024, doi: 10.1016/j.istruc.2024.107166.

[9] J. Chróścielewski, M. Miśkiewicz, Ł. Pyrzowski, and B. Sobczyk, "Damage analysis of tensioning cable anchorage zone of a bridge superstructure, using CDP Abaqus material model", *Archives of Civil Engineering*, vol. 63, no. 3, pp. 3–18, 2017, doi: 10.1515/ace-2017-0025.

[10] L. Ren, B. Zhu, J. Li, and Q. Wang, "A novel model for detecting prestress by external anchor head section of prestressed anchor cables", *Ocean Engineering*, vol. 311, Part 2, art. no. 118978, 2024, doi: 10.1016/j.oceaneng.2024.118978.

[11] S.W. Hou, Y. Zhou, and S.H. Tian, "Force analysis and experimental study of a new anchoring system for CFRP wire strands", *Structures*, vol. 73, art. no. 108414, 2025, doi: 10.1016/j.istruc.2025.108414.

[12] X.D. Shao, R. Pan, H. Zhao, and Z. Shao, "Prestress Loss of a New Vertical Prestressing Anchorage System on Concrete Box-Girder Webs", *Journal of Bridge Engineering*, vol. 19, no. 2, pp. 210–219, 2014, doi: 10.1061/(ASCE)BE.1943-5592.0000522.

[13] X.D. Shao, et al., "Calculation and Measure of Web Vertical Stress Field Using Low Retracting Prestressed Anchorage", *Journal of Highway and Transportation Research and Development*, vol. 26, no. 9, pp. 91–96, 2009 (in Chinese).

[14] X.D. Shao, et al., "Experimental Study of Concrete Stress under Low Retracting Pre-stress Stranded Anchorage", *Journal of Hunan University*, vol. 37, no. 2, pp. 1–5, 2010 (in Chinese).

[15] Y. Zhang, et al., "Study of the Vertical Prestress Loss in Box Girder Webs with Twice-tension Strand", *Journal of Hunan University*, vol. 39, no. 6, pp. 13–18, 2012 (in Chinese).

[16] L. Correia, T. Teixeira, J. Michels, J.A.P.P. Almeida, and J. Sena-Cruz, "Flexural behaviour of RC slabs strengthened with prestressed CFRP strips using different anchorage systems", *Composites Part B: Engineering*, vol. 81, pp. 158–170, 2015, doi: 10.1016/j.compositesb.2015.07.011.

[17] C. Marchão, V. Lúcio, and H.R. Ganz, "Optimization of anchorage corner blisters for posttensioning tendons", *Structural Concrete*, vol. 18, no. 2, pp. 334–348, 2017, doi: 10.1002/suco.201600057.

[18] GB/T 3077-2015 Alloy structure steels. Standards Press of China, 2015 (in Chinese).

[19] GB/T 700-2006 Carbon structural steels. Standards Press of China, 2006 (in Chinese).

[20] TB/T 3193-2016 Anchorage, grip and coupler for prestressing tendons in railway construction. China Railway Publishing House, 2016 (in Chinese).

[21] JT/T 771-2009 Technical conditions for unbonded steel strand stay cable. China Communications Press, 2009 (in Chinese).

Received: 2024-11-16, Revised: 2025-03-01